

## Early star-forming galaxies and the reionization of the Universe

Brant E. Robertson<sup>1</sup>, Richard S. Ellis<sup>1</sup>, James S. Dunlop<sup>2</sup>, Ross J. McLure<sup>2</sup> & Daniel P. Stark<sup>3</sup>

**Star-forming galaxies trace cosmic history. Recent observational progress with the NASA Hubble Space Telescope has led to the discovery and study of the earliest known galaxies, which correspond to a period when the Universe was only ~800 million years old. Intense ultraviolet radiation from these early galaxies probably induced a major event in cosmic history: the reionization of intergalactic hydrogen.**

The frontier in completing the physical story of cosmic history is to understand cosmic reionization—the transformation of neutral hydrogen, mostly located outside galaxies in the intergalactic medium (IGM), into an ionized state. Neutral hydrogen first formed 370,000 years after the Big Bang and released the radiation presently observed as the cosmic microwave background (CMB)<sup>1</sup>. Initially devoid of sources of light, the Universe then entered a period termed the ‘Dark Ages’<sup>2</sup>, which lasted until the first stars formed from overdense clouds of hydrogen gas that cooled and collapsed within early cosmic structures. Observations of distant quasars<sup>3</sup> demonstrate that the IGM has been highly ionized since the Universe was ~1 billion years (Gyr) old, and the transition from a neutral medium is popularly interpreted as being caused by ionizing photons with energies greater than 13.6 eV (wavelength,  $\lambda < 91.2$  nm), generated by primitive stars and galaxies<sup>4</sup> (Fig. 1).

Astronomers wish to confirm the connection between early galaxies and reionization because detailed studies of this period of cosmic history will reveal the physical processes that originally shaped the galaxies of various luminosities and masses we see around us today. Alternative sources of reionizing photons include material collapsing into early black holes that power active galactic nuclei, and decaying elementary particles. Verifying that star-forming galaxies were responsible for cosmic reionization requires understanding how many energetic ultraviolet photons were produced by young stars at early times and what fraction of photons capable of ionizing hydrogen outside galaxies escaped without

being intercepted by clouds of dust and hydrogen within galaxies. Astronomers desire accurate measurements of the abundance of early galaxies and the distribution of their luminosities to quantify the number of sources producing energetic photons, as well as a determination of the mixture of stars, gas and dust in galaxies, to determine the likelihood that the ultraviolet radiation can escape to ionize the IGM<sup>5,6</sup>. The Lyman- $\alpha$  ( $\text{Ly}\alpha$ ) emission line, which is detectable using spectrographs on large ground-based telescopes, is a valuable additional diagnostic given that it is easily erased by neutral gas outside galaxies<sup>7–12</sup>. Its observed strength in distant galaxies is therefore a sensitive gauge of the latest time when reionization was completed.

In this primarily observational Review, we discuss substantial progress that now points towards a fundamental connection between early galaxies and reionization. Recent observations with the Hubble Space Telescope (HST) have provided the first detailed constraints on the abundance and properties of galaxies in the first 1 Gyr of cosmic history. With some uncertainties, these data indicate that sufficient ultraviolet radiation was produced to establish and maintain an ionized Universe by redshift  $z \approx 7$ , corresponding to ~800 million years (Myr) after the Big Bang. Further observations of these early systems using current facilities will produce a more robust census and clarify what fraction of the ionizing radiation escaped primitive galaxies. The rapid progress now being made will pave the way for ambitious observations of the earliest known galaxies using future facilities.

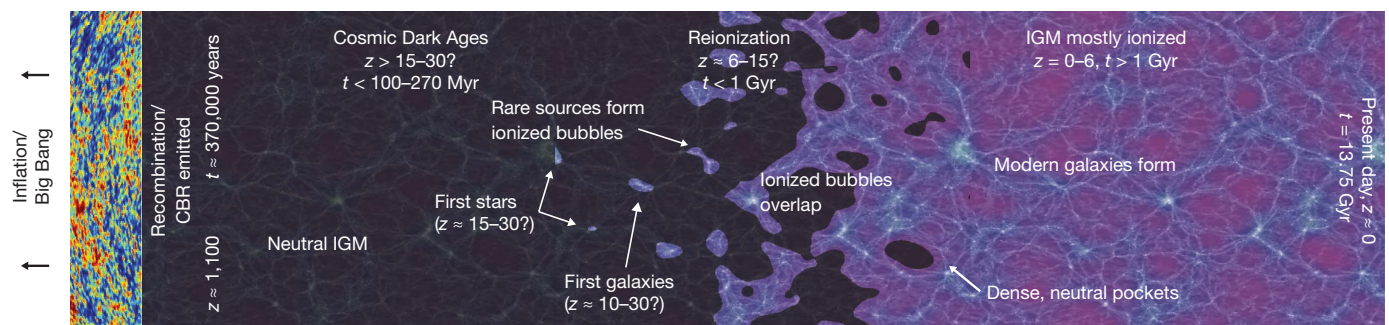


**Figure 1 | Cosmic reionization.** The transition from the neutral IGM left after the Universe recombined, at  $z \approx 1,100$ , to the fully ionized IGM observed today is termed cosmic reionization. After recombination, when the CMB radiation was released, hydrogen in the IGM remained neutral until the first stars and galaxies<sup>2,4</sup> formed, at  $z \approx 15–30$ . These primordial systems released energetic ultraviolet photons capable of ionizing local bubbles of hydrogen gas. As the

abundance of these early galaxies increased, the bubbles increasingly overlapped and progressively larger volumes became ionized. This reionization process ended at  $z \approx 6–8$ , ~1 Gyr after the Big Bang. At lower redshifts, the IGM remains highly ionized by radiation provided by star-forming galaxies and the gas accretion onto supermassive black holes that powers quasars.

<sup>1</sup>Department of Astronomy, California Institute of Technology, MC 249-17, Pasadena, California 91125, USA. <sup>2</sup>Institute for Astronomy, University of Edinburgh, Edinburgh EH9 3HJ, UK. <sup>3</sup>Institute of Astronomy, University of Cambridge, Cambridge CB3 0HA, UK.

## Probes of the reionization epoch

Cosmological reionization involves a complex interplay between the strength, distribution and spectrum of photoionizing sources and the density and spatial structure of intergalactic gas. Theoretical calculations using both analytical methods<sup>13–17</sup> and sophisticated numerical simulations<sup>18–28</sup> to model these complexities have reached broad agreement on how reionization is expected to proceed (Fig. 1). Sources of ionizing photons, such as star-forming galaxies, are associated with dark matter halos forged through hierarchical structure formation<sup>29</sup>. Initially, these sources are rare and only ionize sparse localized ‘bubbles’ in the dense IGM. As the Universe expands and the mean IGM density decreases, early sources grow in abundance, mass and luminosity with time and the ionized regions increase in number and extent. The ionized bubbles eventually overlap, allowing the mean free path of ionizing photons and the average volume fraction of ionized hydrogen,  $Q_{\text{H II}}$ , in the IGM to increase rapidly. The process is completed with the ionization of neutral pockets of hydrogen gas isolated from luminous sources. A technical description of the reionization process and the key requirements for star-forming galaxies to be the responsible agents are provided in Box 1.

The complete ionization of hydrogen in the IGM requires sustained sources of Lyman-continuum photons with wavelengths  $\lambda < 91.2$  nm. If galaxies are responsible, the process of reionization should mirror their

time-dependent density. The number of Lyman-continuum photons produced by star-forming galaxies can be modelled and, assuming that some fraction can escape the galaxies, the average volume fraction of hydrogen ionized by these photons ( $Q_{\text{H II}}$ ) can be calculated from the star formation rate density. The history of star formation is further constrained by its time integral, the mass density of long-lived stars. At high redshift, the presence of such stars is usefully probed by the NASA Spitzer Space Telescope<sup>30,31</sup>. A final constraint is the optical depth for Thomson scattering by free electrons associated with reionization, as inferred by their ability to polarize CMB photons. Observational constraints on the electron optical depth<sup>32</sup> suggest that an extended, low level of ionization ( $\sim 10\%$  by volume) may be needed to high redshifts ( $z > 20$ ) if reionization gradually ends at  $z \approx 5.5$ – $8.5$ . Reconciling the electron scattering optical depth with the number of available ionizing photons inferred from the currently observed star formation rate may therefore be difficult.

The above observations are discussed in more detail in Box 2. These indirect constraints are broadly consistent with a gradual reionization starting at  $z \approx 20$  and ending at  $z \approx 6$ , as first indicated by measures of neutral hydrogen absorption in distant quasar and gamma-ray burst spectra that can probe the end of reionization<sup>33–36</sup>. Ultimately, we may chart the distribution of ionized bubbles forming within intergalactic neutral hydrogen directly using radio interferometers sensitive to the hyperfine transition at 21 cm, but this topic is not covered explicitly here (for a review, see ref. 37). Such technically challenging 21-cm observations are still some years away, but with the newly refurbished HST we can make immediate progress through a direct census of faint star-forming galaxies and studies of their stellar populations.

### A first census of early galaxies

High-redshift galaxies are located by detecting the effect of intervening neutral hydrogen absorption on their colours. Even small amounts of neutral gas can extinguish the light from a galaxy at smaller wavelengths than the Ly $\alpha$  line in its rest frame, causing a ‘break’ in the observed galaxy spectrum. As a result, high-redshift galaxies are often referred to as Lyman-break galaxies<sup>38–41</sup>, and the telltale signature of such a distant object is its disappearance or ‘drop-out’ from an imaging filter sensitive to the redshifted ultraviolet passband where the hydrogen absorption occurs. Identifying the highest-redshift galaxies and determining their influence on reionization therefore require an infrared-sensitive camera.

Excellent progress has been made using the drop-out technique to find high-redshift galaxies since May 2009, following the installation of the HST’s Wide Field Camera 3, a panoramic imager that includes a powerful infrared detector (WFC3/IR) operating in the wavelength range 850–1,700 nm. Taking into account the infrared field of view, pixel scale and efficiency, this instrument provides a 40-fold improvement in survey speed over the previous-generation instrument, the Near Infrared Camera and Multi-Object Spectrometer. The HST Wide Field Camera 3 undertook a series of deep images of the Hubble Ultra Deep Field (UDF; a 4.7-arcmin<sup>2</sup> area) reaching an optimal  $5\sigma$  point source sensitivity of  $\sim 29$ th magnitude in three broadband filters (Box 3). These data, together with shallower exposures in other areas, have provided the first convincing census of  $z \approx 7$  galaxies and initial indications of galaxy populations at yet higher redshifts<sup>39–47</sup>.

The most important result to emerge from the new WFC3/IR data has been the first robust determination of the volume density of galaxies of different luminosities at  $z \approx 7$  (the luminosity function), based on over 50 sources seen so far in the various WFC3/IR campaigns. To these HST data sets can be added constraints based on 22  $z \approx 7$  candidates similarly detected to brighter limits (AB magnitude,  $m_{\text{AB}} \approx 26$ ) using the NAOJ Subaru telescope<sup>48</sup> (Box 3), extending the range of the luminosity function. The depth of the HST images has been particularly advantageous, as the luminosity function increases steeply for intrinsically fainter sources, indicating that the bulk of the ultraviolet luminosity density from star-forming galaxies at  $z \approx 7$  emerges from an abundant population of very faint systems.

#### BOX 1

### The physics of reionization

The process of reionization follows the transition from the neutral IGM, at high redshift, to the ionized IGM we observe locally. The volume ionization fraction of the IGM,  $Q_{\text{H II}}$ , progresses from neutral ( $Q_{\text{H II}} = 0$ ) to fully ionized ( $Q_{\text{H II}} = 1$ ) according to a changing balance between the production rate of ionizing photons and the recombination rate<sup>13–16</sup>. The production rate of IGM-ionizing photons

$$\frac{dn_{\text{ion}}}{dt} = f_{\text{esc}} \zeta_Q \rho_{\text{SFR}}$$

is the product of the co-moving star formation rate density,  $\rho_{\text{SFR}}$  (in units of  $M_{\odot} \text{ yr}^{-1} \text{ Mpc}^{-3}$ , where  $M_{\odot}$  is the solar mass), the number of hydrogen-ionizing photons per second per unit star formation rate,  $\zeta_Q$  ( $\text{s}^{-1} M_{\odot}^{-1} \text{ yr}$ ), and the fraction of photons that can escape a galaxy,  $f_{\text{esc}}$ . The rate  $dn_{\text{ion}}/dt$  is therefore fundamentally tied to the abundance and detailed astrophysics of early stars and galaxies. The recombination rate depends on the IGM temperature and the physical hydrogen density, which decreases with time according to the universal expansion factor,  $a^{-3}$ , and is enhanced in locally overdense regions by the ‘clumping factor’,  $C_{\text{H II}} = \langle n_{\text{H}}^2 \rangle / \langle n_{\text{H}} \rangle^2$ , where  $n_{\text{H}}$  is the hydrogen number density and angle brackets denote a cosmic average. Recent estimates suggest that  $C_{\text{H II}} \approx 1$ – $6$  (refs 16, 85). The recombination rate therefore depends primarily on atomic physics and the details of cosmological structure formation.

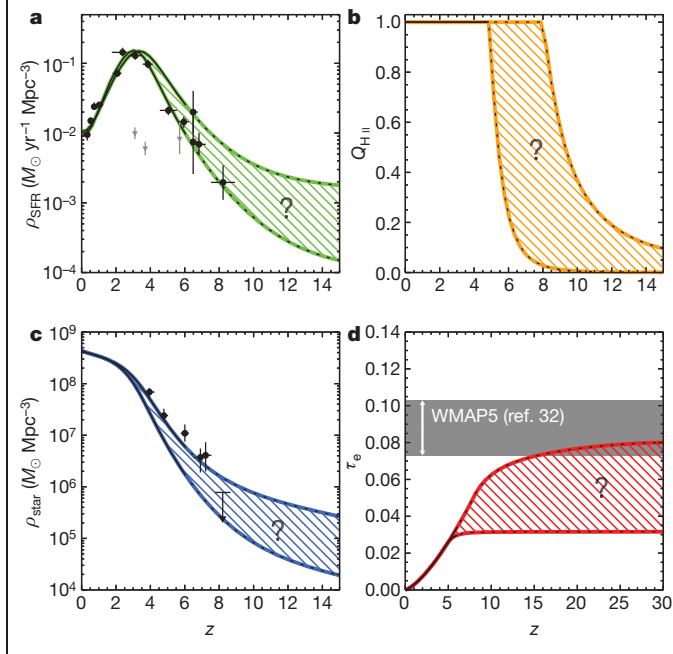
The observational requirements for determining whether galaxies had the dominant role in causing reionization are summarized as follows. First,  $\rho_{\text{SFR}}$  must be quantified, and is typically measured using the observable proxy of the rest-frame ultraviolet luminosity density,  $\rho_{\text{UV}}$ , through the luminosity distribution of high-redshift star-forming galaxies. Second,  $\zeta_Q$  and  $f_{\text{esc}}$  must be observationally estimated by determining the relative effects of stars, dust and nebular emission on the rest-frame ultraviolet region of high-redshift galaxy spectral energy distributions or by direct observations in the Lyman continuum at lower redshift. To reionize the Universe fully, the integrated history of star formation must produce more than one ionizing photon per atom, such that ionizations exceed recombinations. For a standard stellar initial mass function, this requirement can be translated<sup>2</sup> into an effective co-moving stellar mass density of  $\rho_{\text{star}} \approx 2 \times 10^6 f_{\text{esc}}^{-1} M_{\odot} \text{ Mpc}^{-3}$ .

**BOX 2**

## Observational probes of the reionization epoch

The observed rest-frame ultraviolet luminosity density of star-forming galaxies, which are the expected sources of the photons that cause reionization, provides the cosmic star formation rate density,  $\rho_{\text{SFR}}$  (Figure panel **a**: circles with 1-s.d. error bars<sup>40,41,62,86,87</sup>; grey points indicate the contribution from Ly $\alpha$ -emitting galaxies<sup>65</sup>). Also shown are illustrative model star formation histories for typical stellar ages of  $10^8$  yr, which are consistent with these observations (green area) and are based on an extension of the fitting form proposed in ref. 88. The models<sup>51,89</sup> range from very metal-poor stars ( $Z \approx 5 \times 10^{-6} Z_{\odot}$ , where  $Z_{\odot}$  is the solar metallicity), at the upper boundary, to metal-rich stars ( $Z \approx 2Z_{\odot}$ ; see details below). We adopt the form  $\rho_{\text{SFR}}(z) = [a + b(z/c)h] / [1 + (z/c)d] + g$  with  $a = 0.009 M_{\odot} \text{ yr}^{-1} \text{ Mpc}^{-3}$ ,  $b = 0.27 M_{\odot} \text{ yr}^{-1} \text{ Mpc}^{-3}$  and  $h = 2.5$ . In the metal-poor case we take  $c = 3.7$ ,  $d = 7.4$ ,  $g = 10^{-3} M_{\odot} \text{ yr}^{-1} \text{ Mpc}^{-3}$ ,  $f_{\text{esc}} = 0.3$  and  $C_{\text{HII}} = 2$ , and in the metal-rich case we take  $c = 3.4$ ,  $d = 8.3$ ,  $g = 10^{-4} M_{\odot} \text{ yr}^{-1} \text{ Mpc}^{-3}$ ,  $f_{\text{esc}} = 0.2$  and  $C_{\text{HII}} = 6$ .

The volume fraction of ionized hydrogen,  $Q_{\text{HII}}$ , implied by these models is shown in Figure panel **b** (orange region), where, consistent with the present data, the Universe becomes fully reionized ( $Q_{\text{HII}} = 1$ ) at redshifts  $z \approx 5.5$ – $8.5$ . The observed stellar mass density (Figure panel **c**: data points with 1-s.d. error bars<sup>30,31,49–51,90</sup>) also constrains the process of reionization because the stellar mass should trace the integral of the star formation rate density (blue shaded area) if most stars are long lived. Their relative agreement indicates that population III stars may not contribute significantly to the ultraviolet luminosity density at  $z \approx 7$ . Finally, the scattering optical depth,  $\tau_e$ , of free electrons that polarize the CMB can also be measured<sup>32</sup> (Figure panel **d**: grey shaded area). The model  $\tau_e$  (red area) can be calculated from  $Q_{\text{HII}}$  by finding the path length through ionized hydrogen along the line of sight to the CMB. Producing the large electron scattering optical depth given the observed star formation rate density may be difficult without an evolving initial mass function, contribution from population III stars or yet-unobserved star formation at higher redshifts ( $z > 10$ ).



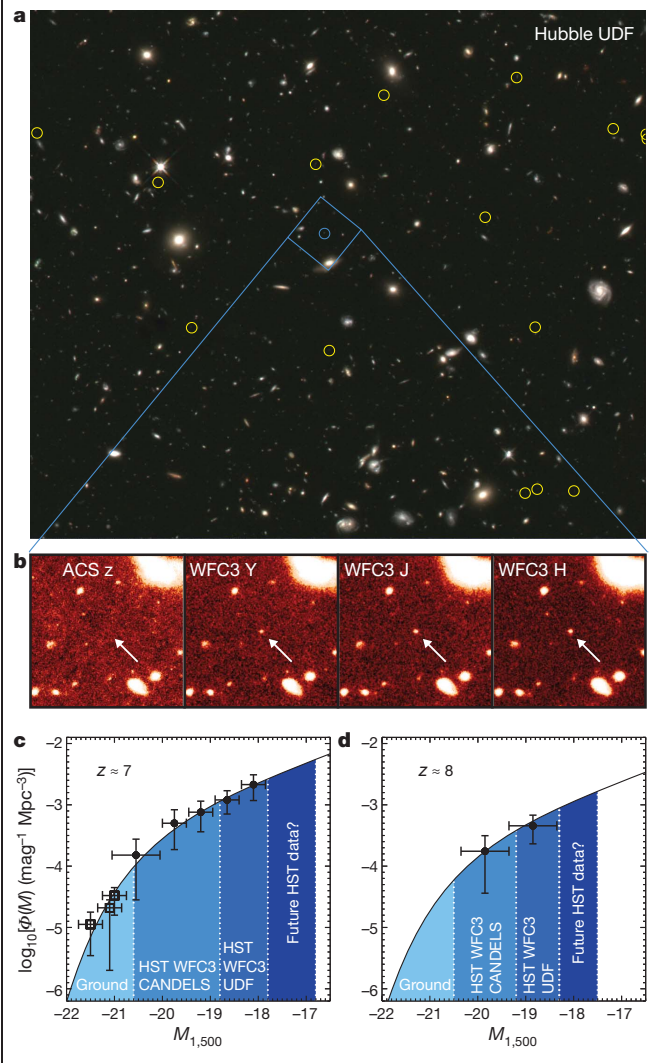
The most luminous  $z \approx 7$  galaxies have also been detected individually by Spitzer<sup>49,50</sup>, and many show strong continua at wavelengths greater than 400 nm in their rest frame, indicating established stellar populations

**BOX 3**

## The discovery and study of galaxies at redshifts $z > 7$

The search for galaxies at extreme redshifts has been revolutionized by the successful installation of the new Wide Field Camera 3 in the HST. Figure panel **a** shows the deepest near-infrared image of the Hubble UDF yet taken with the new WFC3/IR camera, with the positions of newly discovered  $z \approx 7$ – $8$  galaxies<sup>39–41</sup> indicated (circles). For a selected  $z \approx 7$  candidate, Figure panel **b** shows that clear detections in the Y (1.05  $\mu\text{m}$ ), J (1.2  $\mu\text{m}$ ) and H (1.6  $\mu\text{m}$ ) bands with WFC3/IR, combined with the non-detection in the optical z band (0.85  $\mu\text{m}$ ), imaged with the Advanced Camera for Surveys (ACS), yield a secure photometric redshift<sup>39</sup> of  $z = 7.2$ .

The year-one WFC3/IR observations have already produced sufficient numbers of high-redshift galaxies to allow the first reliable determination<sup>39</sup> of the galaxy luminosity function,  $\Phi(M)$ , at  $z = 7$  (Figure panel **c**: circles with 1-s.d. error bars) and an initial estimate at  $z = 8$  (Figure panel **d**: circles with 1-s.d. error bars). Here  $M_{1,500}$  denotes the absolute AB magnitude at 1,500  $\text{\AA}$  in the galaxy rest frame. Large-area ground-based surveys<sup>48</sup> (Figure panel **c**: open squares with 1-s.d. error bars) are required to uncover the rarest luminous objects at the bright end of the luminosity function, and the newly approved HST Multi-Cycle Treasury Program, CANDELS, will provide a few hundred galaxies at luminosities around the characteristic luminosity  $L^*$  at  $z = 7$ – $8$ . More-sensitive imaging in the UDF is possible and is necessary to measure the number densities of fainter galaxies and to extend these studies to  $z \approx 9$ – $10$ .



of  $\sim 10^9$ – $10^{10}$  solar masses. Stacking the Spitzer images of the more abundant, fainter population gives hints of a marginal signal corresponding to similar stellar populations whose mean mass is  $10^8$ – $10^9$  solar masses<sup>51</sup>. The combination of HST and Spitzer has been very effective in addressing the key issue of identifying a sustained source of ionizing radiation. Although uncertainties remain, there is now reasonably convincing evidence that star formation in individual galaxies proceeded at a roughly constant rate over an extended period of 300 Myr, corresponding to the redshift range  $7 < z < 10$ .

### The escape fraction of ionizing photons

In addition to counting the number of galaxies that produce energetic radiation, we must establish whether a sufficient fraction of the associated ultraviolet photons escape to allow reionization. To quantify the production rate of ionizing photons,  $dn_{\text{ion}}/dt$ , and conclusively determine the role of galaxies in cosmic reionization, we thus turn to the problem of determining the number,  $\zeta_Q$ , of energetic Lyman-continuum photons per unit star formation rate produced by early stellar populations, and the fraction,  $f_{\text{esc}}$ , of such photons that freely escape each galaxy (Box 1). Although these quantities almost certainly vary significantly from one galaxy to the next, we can legitimately seek to establish a representative average for the purposes of determining the role of galaxies in reionization.

Because ultraviolet photons that have wavelengths below the Lyman limit (91.2 nm), and are therefore capable of reionizing the intergalactic atoms, are rapidly absorbed by neutral gas in the galaxy, the most direct way of estimating  $f_{\text{esc}}$  is to measure the emerging flux in this wavelength range. Such observations are intrinsically difficult because typically  $f_{\text{esc}} \ll 1$  and the intervening IGM along the line of sight can absorb the escaping photons, further attenuating the detected Lyman-continuum flux. Despite these challenges, spectroscopic and narrow-band imaging observations<sup>52–55</sup> have detected Lyman-continuum flux from galaxies at redshift  $z \approx 3$ , which is the practical redshift limit for this method. These measurements show that the effective escape fraction can vary widely from galaxy to galaxy, but imply characteristic values of  $0.1 \lesssim f_{\text{esc}} \lesssim 0.2$  at  $z \approx 3$ .

The same experiment at redshift  $z \approx 7$  is not technically feasible owing to the increased IGM absorption of high-redshift sources. However, another photometric signature of Lyman-limit photons as they migrate out of a young galaxy might be observable. If such a photon encounters neutral gas in the galaxy, it will probably ionize a portion of that gas and lead to line emission as well as free–free and bound–free scatterings between electrons and protons. These processes produce nebular radiation whose characteristic emission spectrum can be detected. Models incorporating both the stellar and nebular contributions to galactic emission<sup>56,57</sup> predict a spectrum whose power-law slope,  $\beta$  (such that the flux scales with wavelength as  $f(\lambda) \propto \lambda^\beta$ ), is strongly dependent on the number of escaping ionizing photons through  $\zeta_Q$  and  $f_{\text{esc}}$  (ref. 42; Fig. 2). However, unlike the direct measurement of Lyman continuum photons at  $z \approx 3$ , this indirect method of estimating  $f_{\text{esc}}$  from the spectral character of  $z \approx 7$  galaxies has yet to be conclusively demonstrated.

Lower-luminosity galaxies in the redshift range  $4 < z < 7$  have steep ultraviolet slopes<sup>58</sup>,  $\beta < -2.0$ , consistent with the hypothesis that these are relatively dust-free systems<sup>44</sup>. Moreover, the new HST data has now indicated that this trend continues to higher redshift, where ultraviolet slopes with  $\beta < -2.5$  have reportedly been observed<sup>42,44</sup>. Because the youngest starburst galaxies in the local Universe have ultraviolet spectra with  $\beta > -2.5$  (refs 58, 59) and extreme slopes ( $\beta < -3$ ) may indicate population III stars<sup>60,61</sup>, the large negative slope values derived from the new HST data are intriguing.

The ultraviolet slope measurements beyond  $z \approx 7$  remain controversial, partly because of the photometric uncertainties involved. However, if verified with more-precise, deeper imaging, current models suggest that such steep slopes most likely indicate nearly dust-free, metal-poor stellar systems with large  $\zeta_Q$  values or young galaxies with very little nebular spectra, as would be expected if the escape fraction was significant (for

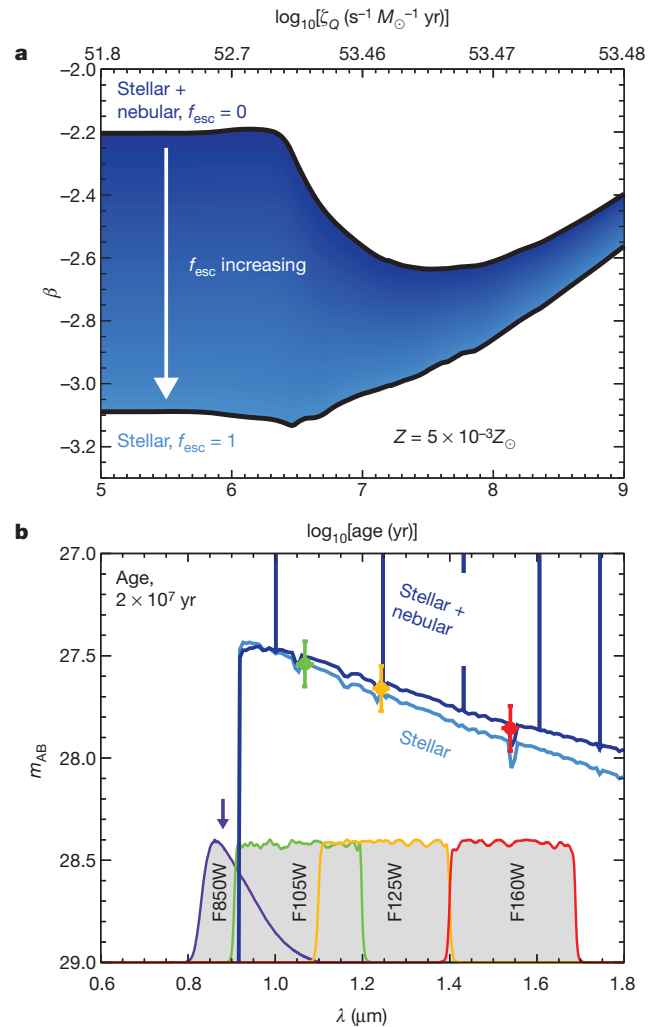


**Figure 2 | Ionizing flux from high-redshift galaxies.** The co-moving flux of hydrogen ionizing photons,  $dn_{\text{ion}}/dt$ , produced by galaxies depends on the total star formation rate density,  $\rho_{\text{SFR}}$ , the number of ionizing photons per unit star formation rate,  $\zeta_Q$ , and the fraction,  $f_{\text{esc}}$ , of these photons that can escape galaxies to ionize the IGM. Most galaxies at  $z \approx 7$  seem to be nearly dust free<sup>42</sup>, and the escape fraction may therefore reflect the internal ionization rate of gas within each galaxy. This internal ionization produces nebular emission<sup>78</sup> that can redden the spectra of nearly metal-free, star-forming galaxies. The colour of the galaxy determined using various filters (shaded areas in **b**) may therefore constrain  $\zeta_Q$  and  $f_{\text{esc}}$  (ref. 57). **a**, Ultraviolet spectral slope,  $\beta$ , defined in terms of the flux density as  $f(\lambda) \propto \lambda^\beta$ , for the case of a metal-poor galaxy. We calculate  $\beta$  from stellar population synthesis models<sup>79,80</sup> and our newly constructed model for the nebular spectrum<sup>78,81–84</sup>. Galaxies with constant star formation rates and  $f_{\text{esc}} \approx 1$  may appear extremely blue, whereas models with  $f_{\text{esc}} \approx 0$  are redder owing to nebular emission. Measuring this slope for  $z \approx 7$  galaxies is difficult. **b**, Model high-redshift galaxy spectra with and without nebular emission, along with the synthesized photometry in the available HST filters (data points). The typical UDF photometric uncertainty is  $\sim 0.25$  mag per source and  $\sim 0.11$  mag for stacked photometry of 20 objects (error bars, 1 s.d.). Hence, the current data are insufficiently deep to infer  $f_{\text{esc}}$  and  $\zeta_Q$  unambiguously from the spectral slope.

example  $f_{\text{esc}} > 0.2$ ). Reliably measuring the ultraviolet slopes for a population of  $z \approx 7$ – $8$  galaxies is within the capabilities of the HST if sufficiently deep exposures are used, and holds the key to constraining the desired combination of  $\zeta_Q$  and  $f_{\text{esc}}$  values.

Our calculations (Fig. 3) find that the  $z \approx 7$  photon budget,  $dn_{\text{ion}}/dt$ , for reionization is already balanced by the observed population of galaxies, although with some uncertainty. However, we show that ongoing, wider-area HST surveys, as well as future, deeper exposures, can resolve the remaining statistical uncertainties. Finalizing the connection between young galaxies and reionization will thus be possible well before the

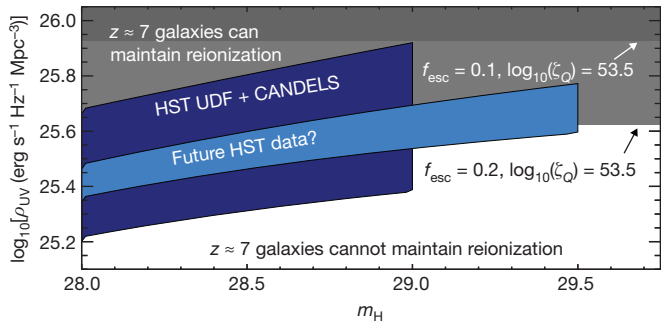


**Figure 3 | Distant star-forming galaxies and reionization.** Expected constraint on  $dn_{\text{ion}}/dt$  from the combined data of the UDF and the forthcoming CANDELS HST surveys, determined using a Fisher matrix calculation<sup>73</sup>. Shown is the  $3\sigma$  uncertainty in the rest-frame ultraviolet luminosity density,  $\rho_{\text{UV}}$  (the observable proxy for  $\rho_{\text{SFR}}$ ; dark blue region), and the improved constraint achieved by increasing the UDF limiting depth by 0.5 mag (light blue region). The light and dark grey regions show the  $\rho_{\text{UV}}$  ranges necessary for ionizations to balance recombinations in the IGM for  $f_{\text{esc}} = 0.2$  and  $f_{\text{esc}} = 0.1$ , respectively, assuming that  $\zeta_Q = 10^{53.5} \text{ s}^{-1} M_{\odot}^{-1} \text{ yr}$  (Fig. 2) and  $C_{\text{HI}} \approx 2$ . Increased  $C_{\text{HI}}$ , decreased  $f_{\text{esc}}$  and decreased  $\zeta_Q$  require correspondingly greater  $\rho_{\text{UV}}$  for ionization–recombination balance. The putative escape fraction values are motivated by the steep observed ultraviolet slopes of  $z \approx 7$  galaxies<sup>42</sup> and detections of Lyman-continuum flux from  $z \approx 3$  galaxies<sup>52–55</sup>. These estimates are calculated using the measured luminosity function power-law faint-end slope<sup>39</sup> of  $\alpha = -1.72$ ; a steeper slope would increase the inferred ultraviolet luminosity density and ionizing flux produced by galaxies. The depth of the UDF and the large area of CANDELS will constrain the abundance of  $z \approx 7$  galaxies well enough to evaluate the hypothesis that galaxies trigger reionization, but a definitive test of this will require deeper data in the UDF with a commitment of additional exposure time comparable to the previous effort. With its new WFC3/IR instrument, the HST is capable of performing this experiment in the near future.  $m_{\text{H}}$ , AB magnitude in the H band.

arrival of the new facilities that will study this important reionization era in greater detail.

### Charting the end of reionization

Just as quasars were originally used as distant beacons to probe the IGM at low redshift, the spectroscopy of distant galaxies can test for the presence of neutral hydrogen along the line of sight. A valuable spectral diagnostic in distant star-forming galaxies is the Ly $\alpha$  emission line at rest wavelength of 121.6 nm, which is produced internally by gas heated by young stars. The observability of Ly $\alpha$  emission is sensitive to the ionization state of the IGM, as the observed line strength can be attenuated by intervening neutral hydrogen. The challenge to using this technique to chart the end of reionization lies in isolating the impact of neutral hydrogen from other effects that may diminish the strength of the Ly $\alpha$  line, including dust.

The abundance of drop-out-selected galaxies decreases markedly from redshifts  $z \approx 3$  to  $\sim 7$  (ref. 62), yet the fraction of these galaxies showing intense Ly $\alpha$  emission increases with redshift<sup>63</sup>. An important complementary technique for selecting high-redshift Ly $\alpha$  emitting galaxies<sup>64</sup> through narrowband filters yields a similar result<sup>65</sup> (Fig. 4a). As the strong line emitters are generally found to be galaxies with dust-free colours, the increasing fraction of line emitters suggests a reduced obscuration by dust at early times. We therefore expect most early star-forming galaxies to exhibit prominent Ly $\alpha$  emission, until we reach the era when the IGM became partly neutral, at which point the fraction of line-emitting galaxies should decrease.

Searches for a decrease in the fraction of Ly $\alpha$ -emitting galaxies could thus be a very effective probe of when reionization ended<sup>17,9,10</sup>. Much excitement has been generated by a claimed drop in the abundance of Ly $\alpha$  emitters seen in narrowband imaging surveys with the Subaru telescope<sup>66</sup> in the short time interval (150 Myr) between  $z = 5.7$  and 6.6. Further studies of a larger area<sup>67</sup> at  $z = 6.6$  and a deeper narrowband search<sup>68</sup> at  $z = 7$  also indicate a decreasing abundance of Ly $\alpha$ -emitting galaxies at  $z > 6.5$ . Such a change might highlight an increase in the IGM

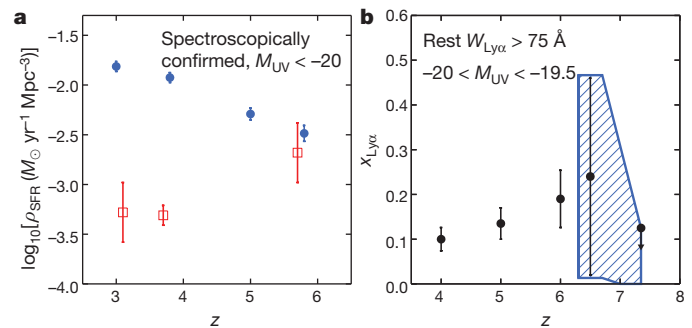


**Figure 4 | Tracing the end of reionization with the Ly $\alpha$  line.** **a**, Recent observations have revealed that the abundance of narrowband-selected Ly $\alpha$ -emitting galaxies (LAEs, red squares) is increasing<sup>65</sup> for  $3 < z < 6$ , when the IGM is known to be highly ionized, whereas the abundance of colour-selected Lyman-break galaxies (LBGs, blue points) is decreasing<sup>62</sup>. In the absence of changes in the IGM ionization state, we therefore expect most dust-free  $z > 6$  galaxies to show powerful Ly $\alpha$  line emission. **b**, Observations at  $z > 6$  have instead revealed a possible decrease in the prevalence of Ly $\alpha$  emitters<sup>66</sup> for  $5.7 < z < 7.0$  (black points), as expected if reionization ended at  $z \approx 6$ . This trend may now be confirmed by spectroscopic surveys of  $4 < z < 7$  LBGs that show a tentative decrease in the fraction of Ly $\alpha$ -emitting galaxies<sup>63,70,71</sup> at  $z > 6.3$  (blue hatched region). This result will require confirmation through infrared spectroscopy of  $z > 7$  LBGs. Error bars, 1 s.d.  $M_{\text{UV}}$ , absolute magnitude in the ultraviolet;  $W_{\text{Ly}\alpha}$ , Ly $\alpha$  equivalent width;  $x_{\text{Ly}\alpha}$ , fraction of sample showing Ly $\alpha$  emission with  $W_{\text{Ly}\alpha} > 75 \text{ \AA}$ .

neutral fraction. The patchy character of the neutral IGM at the end of reionization should also affect the spatial clustering of Ly $\alpha$  emitters<sup>69</sup>, but as no such signal has been detected the question of whether this drop arises from a change in IGM transmission remains unanswered.

To verify the potentially important decrease in the abundance of Ly $\alpha$  emitters beyond  $z \approx 6$ , the fraction of line-emitting galaxies needs to be determined at even earlier times. If the Subaru survey results arose from an increased neutral fraction, we would expect a continued drop in the fraction of line-emitting galaxies at higher redshift. A few  $z \approx 7$ –8 gravitationally lensed Lyman-break candidates have been found using deep imaging in foreground massive clusters, but none has been spectroscopically confirmed<sup>70,71</sup> and, thus, some candidates may be at lower redshift. However, intriguingly, no Ly $\alpha$  emission has been seen in any of these lensed sources, suggesting that there has been a continued increase in the neutral fraction (Fig. 4b). Recently, there has been a claimed spectroscopic detection of Ly $\alpha$  line emission from a  $z = 8.6$  drop-out-selected galaxy<sup>72</sup> found in the new HST data. If confirmed, the detection of a Ly $\alpha$  line emitter would be a milestone in the study of the state of the IGM during the reionization epoch. Extending the Ly $\alpha$  visibility test with other  $z > 7$  candidates newly discovered by HST is therefore an important priority for which results can be expected soon.

### Future prospects

Although the rapid advances in the study of the reionization epoch afforded by the new capabilities of the HST have been remarkable, a variety of outstanding observational issues remain. Accurate measures of the abundance of high-redshift galaxies and their luminosity distributions may still need to be improved, and a detailed study of the stellar populations in these galaxies is necessary to predict their output of ultraviolet photons robustly. Furthermore, the gaseous content of high-redshift galaxies and the structure of neutral hydrogen in the IGM external to these galaxies are largely unknown. Addressing these outstanding issues will require renewed effort at existing and forthcoming observatories over the next decade.

We argue that the HST can further exploit its new infrared capabilities to improve the census of high-redshift galaxies. The current limitations are the precision with which the faint-end slope,  $\alpha$ , of the luminosity function is determined and the possibility of contamination from lower-redshift sources. We have carefully evaluated various survey strategies<sup>73</sup>

and estimate that a now-approved, larger-area, multicycle HST survey, in combination with the deeper UDF exposures, will improve the bright end of the luminosity function and reduce the uncertainty in  $\alpha$  to  $\pm 0.15$ . These observations will provide more-precise estimates of the overall ultraviolet luminosity and star formation rate densities. Further deep HST imaging resulting from an investment comparable to that made for the current UDF data would improve the uncertainty in  $\alpha$  to  $\pm 0.08$  (Fig. 3). Such ultra-deep exposures, with a deployment of infrared filters carefully arranged to tighten constraints on the ultraviolet slopes of  $z \approx 7$  galaxies, can also be used to identify higher-redshift galaxies reliably.

Detailed spectroscopic studies of the stellar populations of high-redshift galaxies are required to determine the abundance of young, hot stars and the importance of the gas and dust in absorbing photons that can reionize the IGM. Although comparable sources at lower redshift may soon be within reach of a new generation of infrared spectrographs nearing completion for 8–10-m-class telescopes, the NASA James Webb Space Telescope<sup>74</sup> (JWST) and the next generation of extremely large ground-based telescopes with apertures of 20–40 m (the Thirty Meter Telescope<sup>75</sup>, the Giant Magellan Telescope<sup>76</sup> and the ESO European Extremely Large Telescope (<http://www.eso.org/public/teles-instr/e-elt.html>)) will ultimately resolve observational uncertainties about whether strong nebular emission pollutes some of the Spitzer photometry of  $z \approx 7$  galaxies. If so, both the currently derived stellar masses and ages of high-redshift galaxies have been overestimated<sup>56,57</sup>. Additionally, the JWST will use infrared cameras and spectrographs designed to probe the rest-frame ultraviolet and optical emission from galaxies beyond redshifts  $z \approx 10$ .

Forthcoming radio telescopes will give us information on the abundance and distribution of gas fuelling star formation in high-redshift galaxies, as well as the ionization state of hydrogen in the IGM. The Atacama Large Millimeter/submillimeter Array (<http://www.almaobservatory.org/>) may observe fine-structure carbon and nitrogen lines<sup>77</sup> in distant star-forming galaxies, allowing us to characterize how gas converts into the stars that produce ionizing photons. Future 21-cm interferometers (the Low Frequency Array (<http://www.lofar.org/>), the Murchison Widefield Array (<http://www.mwatelescope.org/>) and the Square Kilometre Array (<http://www.skatelescope.org/>)) have reionization studies as an important scientific justification, and will observe the topology of reionization through the spectral signatures of redshifted neutral hydrogen. These observatories will observe neutral hydrogen in the IGM ‘disappear’ as it is ionized during the reionization process, thereby providing an ‘inverse’ experiment to complement rest-frame ultraviolet observations with the HST and the JWST. As these observational facilities come online over the next decade, the reionization epoch will be thoroughly examined.

1. Penzias, A. A. & Wilson, R. W. A measurement of excess antenna temperature at 4080 Mc/s. *Astrophys. J.* **142**, 419–421 (1965).
2. Loeb, A. *How Did the First Stars and Galaxies Form?* (Princeton Univ. Press, 2010).
3. Gunn, J. E. & Peterson, B. A. On the density of neutral hydrogen in intergalactic space. *Astrophys. J.* **142**, 1633–1641 (1965).
4. Bromm, V., Yoshida, N., Hernquist, L. & McKee, C. F. The formation of the first stars and galaxies. *Nature* **459**, 49–54 (2009).  
**This is an excellent review of the formation of the first stars and galaxies preceding the epoch of reionization.**
5. Gnedin, N. Y., Kravtsov, A. V. & Chen, H.-W. Escape of ionizing radiation from high-redshift galaxies. *Astrophys. J.* **672**, 765–775 (2008).
6. Razoumov, A. O. & Sommer-Larsen, J. Ionizing radiation from  $z = 4$ –10 galaxies. *Astrophys. J.* **710**, 1239–1246 (2010).
7. Miralda-Escude, J. Reionization of the intergalactic medium and the damping wing of the Gunn-Peterson trough. *Astrophys. J.* **501**, 15–22 (1998).
8. Loeb, A. & Rybicki, G. B. Scattered Lyman alpha radiation around sources before cosmological reionisation. *Astrophys. J.* **524**, 527–535 (1999).
9. Santos, M. R. Probing reionization with Lyman  $\alpha$  emission lines. *Mon. Not. R. Astron. Soc.* **349**, 1137–1152 (2004).
10. Malhotra, S. & Rhoads, J. E. Luminosity functions of Ly $\alpha$  emitters at redshifts  $z = 6.5$  and  $z = 5.7$ : evidence against reionization at  $z \leq 6.5$ . *Astrophys. J.* **617**, L5–L8 (2004).
11. Dijkstra, M., Haiman, Z. & Spaans, M. Lyman alpha radiation from collapsing protogalaxies. I. Characteristics of the emergent spectrum. *Astrophys. J.* **649**, 14–36 (2006).
12. Zheng, Z., Cen, R., Trac, H. & Miralda-Escude, J. Radiative transfer modelling of Lyman alpha emitters. I. Statistics of spectra and luminosity. *Astrophys. J.* **716**, 574–598 (2010).
13. Madau, P., Haardt, F. & Rees, M. J. Radiative transfer in a clumpy universe. III. The nature of cosmological ionizing sources. *Astrophys. J.* **514**, 648–659 (1999).

14. Wyithe, J. S. B. & Loeb, A. Reionization of hydrogen and helium by early stars and quasars. *Astrophys. J.* **586**, 693–708 (2003).
15. Choudhury, T. R. & Ferrara, A. Experimental constraints on self-consistent reionization models. *Mon. Not. R. Astron. Soc.* **361**, 577–594 (2005).
16. Bolton, J. S. & Haehnelt, M. G. The observed reionization rate of the intergalactic medium and the ionizing emissivity at  $z \geq 5$ : evidence for a photon-starved and extended epoch of reionization. *Mon. Not. R. Astron. Soc.* **382**, 325–341 (2007).  
**This is a thorough analysis of the ionizing photon budget required for reionization calculated before the new high-redshift HST data was available.**
17. Miralda-Escude, J., Haehnelt, M. & Rees, M. J. Reionization of the inhomogeneous Universe. *Astrophys. J.* **530**, 1–16 (2000).
18. Furlanetto, S. R., Zaldarriaga, M. & Hernquist, L. The growth of H II regions during reionization. *Astrophys. J.* **613**, 1–15 (2005).
19. Gnedin, N. Y. & Fan, X. Cosmic reionization redux. *Astrophys. J.* **648**, 1–6 (2006).
20. Iliev, I. T. *et al.* Simulating cosmic reionization at large scales – I. The geometry of reionization. *Mon. Not. R. Astron. Soc.* **369**, 1625–1638 (2006).
21. McQuinn, M. *et al.* The morphology of H II regions during reionization. *Mon. Not. R. Astron. Soc.* **377**, 1043–1063 (2007).
22. Mesinger, A. & Furlanetto, S. Efficient simulations of early structure formation and reionization. *Astrophys. J.* **669**, 663–675 (2007).
23. Trac, H., Cen, R. & Loeb, A. Imprint of inhomogeneous hydrogen reionization on the temperature distribution of the intergalactic medium. *Astrophys. J.* **689**, L81–L84 (2008).
24. Aubert, D. & Teyssier, R. A radiative transfer scheme for cosmological reionization based on a local Eddington tensor. *Mon. Not. R. Astron. Soc.* **387**, 295–307 (2008).
25. Thomas, R. M. *et al.* Fast large-scale reionization simulations. *Mon. Not. R. Astron. Soc.* **393**, 32–48 (2009).
26. Finlator, K., Ozel, F. & Dave, R. A new moment method for continuum radiative transfer in cosmological reionization. *Mon. Not. R. Astron. Soc.* **393**, 1090–1106 (2009).
27. Choudhury, T. R., Haehnelt, M. G. & Regan, J. Inside-out or outside-in: the topology of reionization in the photon-starved regime suggested by Ly $\alpha$  forest data. *Mon. Not. R. Astron. Soc.* **394**, 960–977 (2009).
28. Alvarez, M. A., Busha, M., Abel, T. & Wechsler, R. Connecting reionization to the local universe. *Astrophys. J.* **703**, 167–171 (2009).
29. Springel, V. *et al.* Simulations of the formation, evolution and clustering of galaxies and quasars. *Nature* **435**, 629–636 (2005).
30. Eyles, L. P. *et al.* The stellar mass density at  $z \approx 6$  from Spitzer imaging of  $i'$ -drop galaxies. *Mon. Not. R. Astron. Soc.* **374**, 910–930 (2007).
31. Stark, D. P., Bunker, A. J., Ellis, R. S., Eyles, L. P. & Lacy, M. A new measurement of the stellar mass density at  $z \approx 5$ : implications for the sources of cosmic reionization. *Astrophys. J.* **659**, 84–97 (2007).
32. Komatsu, E. *et al.* Five-year Wilkinson Microwave Anisotropy Probe (WMAP) observations: cosmological interpretation. *Astrophys. J. Suppl. Ser.* **180**, 330–376 (2009).
33. Fan, X. *et al.* Evolution of the ionizing background and the epoch of reionization from the spectra of  $z \approx 6$  quasars. *Astron. J.* **123**, 1247–1257 (2002).
34. Fan, X., Carilli, C. L. & Keating, B. Observational constraints on cosmic reionization. *Annu. Rev. Astron. Astrophys.* **44**, 415–462 (2006).
35. Becker, G. D., Rauch, M. & Sargent, W. L. W. The evolution of optical depth in the Lyman alpha forest: evidence against reionization at  $z \approx 6$ . *Astrophys. J.* **662**, 72–93 (2007).
36. Kawai, N. *et al.* An optical spectrum of the afterglow of a  $\gamma$ -ray burst at a redshift of  $z = 6.295$ . *Nature* **440**, 184–186 (2006).
37. Furlanetto, S. R., Oh, S. P. & Briggs, F. H. Cosmology at low frequencies: the 21 cm transition and the high-redshift universe. *Phys. Rep.* **433**, 181–301 (2006).
38. Steidel, C. C., Pettini, M. & Hamilton, D. Lyman limit imaging of high-redshift galaxies. III. New observations of four QSO fields. *Astron. J.* **110**, 2519–2536 (1995).
39. McLure, R. J. *et al.* Galaxies at  $z = 6$ –9 from the WFC3/IR imaging of the Hubble Ultra Deep Field. *Mon. Not. R. Astron. Soc.* **403**, 960–983 (2010).  
**This is an early analysis of the abundance of  $z \approx 6$ –9 galaxies and the first combined estimate of the galaxy luminosity function at  $z \approx 7$ –8, as measured from the first release of HST Wide Field Camera 3 data.**
40. Bouwens, R. J. *et al.* Discovery of  $z \approx 8$  galaxies in the Hubble Ultra Deep Field from ultra-deep WFC3/IR observations. *Astrophys. J.* **709**, L133–L137 (2010).
41. Oesch, P. A. *et al.*  $z \approx 7$  galaxies in the HUDF: first epoch WFC3/IR results. *Astrophys. J.* **709**, L16–L20 (2010).  
**This paper gives an initial estimate of the  $z \approx 7$  luminosity function from the early-release HST data.**
42. Bouwens, R. J. *et al.* Very blue UV-continuum slope  $\beta$  of low luminosity  $z \approx 7$  galaxies from WFC3/IR: evidence for extremely low metallicities? *Astrophys. J.* **708**, L69–L73 (2010b).  
**This paper presents the first spectral indication that  $z \approx 7$  galaxies contain young, metal-poor and nearly dust-free stellar populations.**
43. Oesch, P. A. *et al.* Structure and morphologies of  $z \approx 7$ –8 galaxies from ultra-deep WFC3/IR imaging of the Hubble Ultra-Deep Field. *Astrophys. J.* **709**, L21–L25 (2010).
44. Bunker, A. *et al.* The contribution of high redshift galaxies to cosmic reionisation: new results from deep WFC3 imaging of the Hubble Ultra Deep Field. *Mon. Not. R. Astron. Soc.* (in the press); preprint at (<http://arxiv.org/abs/0909.2255>) (2009).
45. Yan, H. *et al.* Galaxy formation in the reionization epoch as hinted by Wide Field Camera 3 observations of the Hubble Ultra Deep Field. *Res. Astron. Astrophys.* **10**, 867 (2010).
46. Wilkins, S. M. *et al.* Probing L\* Lyman-break galaxies at  $z \approx 7$  in GOODS-South with WFC3 on HST. *Mon. Not. R. Astron. Soc.* **403**, 938–944 (2010).
47. Finkelstein, S. L. *et al.* On the stellar populations and evolution of star-forming galaxies at  $6.3 < z < 8.6$ . *Astrophys. J.* **719**, 1250–1273 (2010).

48. Ouchi, M. *et al.* Large area survey for  $z \sim 7$  galaxies in SDF and GOODS-N: implications for galaxy formation and cosmic reionization. *Astrophys. J.* **706**, 1136–1151 (2009).
49. Gonzalez, V. *et al.* The stellar mass density and specific star formation rate of the universe at  $z \sim 7$ . *Astrophys. J.* **713**, 115–130 (2010).
50. Labbe, I., Bouwens, R. J., Illingworth, G. D. & Franx, M. Spitzer IRAC confirmation of  $z_{850}$ -dropout galaxies in the Hubble Ultra Deep Field: stellar masses and ages at  $z \sim 7$ . *Astrophys. J.* **649**, L67–L70 (2006).
- This paper reports Spitzer infrared detections of the recent HST candidates at  $z \approx 7$  indicating the likelihood of earlier star formation.**
51. Labbe, I. *et al.* Ultradeep Infrared Array Camera observations of sub- $L^*$   $z \sim 7$  and  $z \sim 8$  galaxies in the Hubble Ultra Deep Field: the contribution of low-luminosity galaxies to the stellar mass density and reionization. *Astrophys. J.* **708**, L26–L31 (2010).
52. Bunker, A., Marleau, F. & Graham, J. R. Seeking the ultraviolet ionizing background at  $z \sim 3$  with the Keck telescope. *Astron. J.* **116**, 2086–2093 (1998).
53. Steidel, C., Pettini, M. & Adelberger, K. Lyman-continuum emission from galaxies at  $z \approx 3.4$ . *Astrophys. J.* **546**, 665–671 (2001).
54. Shapley, A. *et al.* The direct detection of Lyman continuum emission from star-forming galaxies at  $z \sim 3$ . *Astrophys. J.* **651**, 688–703 (2006).
55. Iwata, I. *et al.* Detections of Lyman continuum from star-forming galaxies at  $z \sim 3$  through Subaru/Suprime-Cam narrow-band imaging. *Astrophys. J.* **692**, 1287–1293 (2009).
56. Schaerer, D. & de Barros, S. The impact of nebular emission on the ages of  $z \approx 6$  galaxies. *Astron. Astrophys.* **502**, 423–426 (2009).
57. Schaerer, D. & de Barros, S. On the physical properties of  $z \sim 6$ –8 galaxies. *Astron. Astrophys.* **515**, 73–88 (2010).
58. Bouwens, R. J. *et al.* UV continuum slope and dust obscuration from  $z \sim 6$  to  $z \sim 2$ : the star formation rate density at high redshift. *Astrophys. J.* **705**, 936–961 (2009).
59. Meurer, G. R., Heckman, T. M. & Calzetti, D. Dust absorption and the ultraviolet luminosity density at  $z \sim 3$  as calibrated by local starburst galaxies. *Astrophys. J.* **521**, 64–80 (1999).
60. Bromm, V., Kudritzki, R. P. & Loeb, A. Generic spectrum and ionization efficiency of a heavy initial mass function for the first stars. *Astrophys. J.* **552**, 464–472 (2001).
61. Schaerer, D. The transition from population III to normal galaxies: Ly  $\alpha$  and He II emission and the ionising properties of high redshift starburst galaxies. *Astron. Astrophys.* **397**, 527–538 (2003).
62. Bouwens, R. J., Illingworth, G. D., Franx, M. & Ford, H. UV luminosity functions at  $z \sim 4, 5$ , and 6 from the Hubble Ultra Deep Field and other deep Hubble Space Telescope ACS fields: evolution and star formation history. *Astrophys. J.* **670**, 928–958 (2007).
- This is a comprehensive analysis of HST data indicating a decrease in the abundance of star-forming galaxies at  $z > 4$ .**
63. Stark, D. P., Ellis, R. S., Chiu, K., Ouchi, M. & Bunker, A. Keck spectroscopy of faint  $3 < z < 7$  Lyman break galaxies: - I. New constraints on cosmic reionisation from the luminosity and redshift-dependent fraction of Lyman-alpha emission. *Mon. Not. R. Astron. Soc.* (in the press); preprint at (<http://arxiv.org/abs/1003.5244>) (2010).
- This paper discusses the visibility of Ly $\alpha$  line emission in galaxies as a tracer of the end of reionization.**
64. Iye, M. *et al.* A galaxy at a redshift  $z = 6.96$ . *Nature* **443**, 186–188 (2006).
65. Ouchi, M. *et al.* The Subaru/XMM-Newton Deep Survey (SXDS). IV. Evolution of Lyman-alpha emitters from  $z = 3.1$  to 5.7 in the  $1 \text{ deg}^2$  field: luminosity functions and AGN. *Astrophys. J. Suppl. Ser.* **176**, 301–330 (2008).
66. Kashikawa, N. *et al.* The end of the reionization epoch probed by Lyman-alpha emitters at  $z = 6.5$  in the Subaru Deep Field. *Astrophys. J.* **648**, 7–22 (2006).
- This paper contains the first intriguing claim of a decrease in the abundance of Ly $\alpha$  emitters, possibly indicative of the end of the reionization epoch.**
67. Ouchi, M. *et al.* Statistics of 207 Ly $\alpha$  emitters at a redshift near 7: constraints on reionization and galaxy formation models. *Astrophys. J.* (in the press); preprint at (<http://arxiv.org/abs/1007.2961>) (2010).
68. Ota, K. *et al.* Lyman alpha emitters at  $z = 7$  in the Subaru/XMM-Newton Deep Survey Field: photometric candidates and luminosity function. *Astrophys. J.* **722**, 803 (2010).
69. McQuinn, M. *et al.* Studying reionization with Ly $\alpha$  emitters. *Mon. Not. R. Astron. Soc.* **381**, 75–96 (2007).
70. Richard, J. *et al.* A Hubble and Spitzer Space Telescope survey for gravitationally lensed galaxies: further evidence for a significant population of low-luminosity galaxies beyond  $z = 7$ . *Astrophys. J.* **685**, 705–724 (2008).
71. Kneib, J.-P., Ellis, R. S., Santos, M. R. & Richard, J. A probable  $z \sim 7$  galaxy strongly lensed by the rich cluster A2218: exploring the dark ages. *Astrophys. J.* **607**, 697–703 (2004).
72. Lehnert, M. D. *et al.* Spectroscopic confirmation of a galaxy at redshift  $z = 8.6$ . *Nature* (in the press).
73. Robertson, B. E. Estimating luminosity function constraints from high-redshift galaxy surveys. *Astrophys. J.* **713**, 1266–1281 (2010).
- This paper presents a statistical formalism for forecasting constraints from high-redshift galaxy surveys that incorporates uncertainty from cosmic variance.**
74. Gardner, J. P. *et al.* The James Webb Space Telescope. *Space Sci. Rev.* **123**, 485–606 (2006).
75. TMT Science Advisory Committee. *Thirty Meter Telescope Detailed Science Case 2007* (<http://www.tmt.org/sites/default/files/TMT-DSC-2007-R1.pdf>) (TMT Observatory Corporation, 2007).
76. GMTO Corporation. *Giant Magellan Telescope Science Requirements* ([http://www.gmto.org/sciencecase/GMT-ID-01405-GMT\\_Science\\_Requirements.pdf](http://www.gmto.org/sciencecase/GMT-ID-01405-GMT_Science_Requirements.pdf)) (Giant Magellan Telescope Organization Corporation, 2006).
77. Walter, F. & Carilli, C. Detecting the most distant ( $z > 7$ ) objects with ALMA. *Astrophys. Space Sci.* **313**, 313–316 (2008).
78. Osterbrock, D. E. & Ferland, G. J. *Astrophysics of Gaseous Nebulae and Active Galactic Nuclei* 2nd edn, 67–91 (Univ. Sci. Books, 2006).
79. Bruzual, G. & Charlot, S. Stellar population synthesis at the resolution of 2003. *Mon. Not. R. Astron. Soc.* **344**, 1000–1028 (2003).
80. Chabrier, G. Galactic stellar and substellar initial mass function. *Publ. Astron. Soc. Pacif.* **115**, 763–795 (2003).
81. Karzas, W. J. & Latter, R. Electron radiative transitions in a Coulomb field. *Astrophys. J.* **6** (suppl.), 167–212 (1961).
82. Brown, R. L. & Mathews, W. G. Theoretical continuous spectra of gaseous nebulae. *Astrophys. J.* **160**, 939–946 (1970).
83. Sutherland, R. S. Accurate free-free Gaunt factors for astrophysical plasmas. *Mon. Not. R. Astron. Soc.* **300**, 321–330 (1998).
84. Anders, P., & Fritze-v. Alvensleben, U. Spectral and photometric evolution of young stellar populations: the impact of gaseous emission at various metallicities. *Astron. Astrophys.* **401**, 1063–1070 (2003).
85. Pawlik, A., Schaye, J. & van Scherpenzeel, E. Keeping the Universe ionised: photoheating and the high-redshift clumping factor of the intergalactic medium. *Mon. Not. R. Astron. Soc.* **394**, 1812–1824 (2009).
86. Schiminovich, D. *et al.* The GALEX-VVDS measurement of the evolution of the far-ultraviolet luminosity density and the cosmic star formation rate. *Astrophys. J.* **619**, L47–L50 (2005).
87. Reddy, N. A. & Steidel, C. C. A steep faint-end slope of the UV luminosity function at  $z \sim 2$ –3: implications for the global stellar mass density and star formation rate in low-mass halos. *Astrophys. J.* **692**, 778–803 (2009).
88. Cole, S. *et al.* The 2dF galaxy redshift survey: near-infrared galaxy luminosity functions. *Mon. Not. R. Astron. Soc.* **326**, 255–273 (2001).
89. Salpeter, E. E. The luminosity function and stellar evolution. *Astrophys. J.* **121**, 161–167 (1955).
90. Stark, D. P. *et al.* The evolutionary history of Lyman break galaxies between redshift 4 and 6: observing successive generations of massive galaxies in formation. *Astrophys. J.* **697**, 1493–1511 (2009).

**Acknowledgements** We thank A. Klypin for the use of his cosmological simulation, and A. Loeb, A. Shapley and L. Hernquist for comments. B.E.R. acknowledges support from a Hubble Fellowship. R.S.E. acknowledges the hospitality of Leiden Observatory. J.S.D. acknowledges the support of the Royal Society through a Wolfson Research Merit award, and also the support of the European Research Council through the award of an Advanced Grant. R.J.M. acknowledges the support of the Royal Society through a University Research Fellowship. D.P.S. acknowledges financial support from an STFC postdoctoral research fellowship and a Schlumberger Research Fellowship at Darwin College.

**Author Contributions** B.E.R. and R.S.E. wrote the main manuscript text. B.E.R. performed the calculations presented in Box 2 and Figs 1–3. J.S.D. and R.J.M. prepared and analysed the data presented in Box 3. D.P.S. prepared and analysed the data presented in Fig. 4. All authors reviewed, discussed and commented on the manuscript.

**Author Information** Reprints and permissions information is available at [www.nature.com/reprints](http://www.nature.com/reprints). The authors declare no competing financial interests. Readers are welcome to comment on the online version of this article at [www.nature.com/nature](http://www.nature.com/nature). Correspondence should be addressed to B.E.R. ([brant@astro.caltech.edu](mailto:brant@astro.caltech.edu)).